Design of Cryogenic Helium Gas Circulation with Multiple Cryocoolers for Superconducting Power Devices

N.G. Suttell[2], C.H. Kim[1], J. Ordonez[2], S. Pamidi[2]

[1]Center for Advanced Power Systems, Tallahassee, FL 32310
[2]FAMU-FSU College of Engineering, Florida State University, Tallahassee, FL 32310

ABSTRACT

Finite element analysis using COMSOL MultiPhysics® is used to study the relative performance of the various potential configurations for multiple units of cryogenic helium circulation systems. The design of large cryogenic systems needed for superconducting power devices require large mass flow rates with significant pressure drops. The models were used to identify the best configuration for an application that operates at around 50 K and requires a helium gas mass flow rate of 12 g/s with a pressure drop of 20 kPa. The configuration with two sets of two parallel circulators is shown to be the best option. The utility of the modeling techniques in the design of a large cryogenic helium circulation systems is demonstrated.

INTRODUCTION

Many High Temperature Superconducting (HTS) power devices have been successfully demonstrated to validate their capabilities and utility in the electric power grid [1]-[16]. The cryogenic systems used in the demonstrations are complex and expensive. Simpler, rugged, and operationally less expensive versions of the cryogenic systems are necessary for realizing the dream of safe, secure, and environmentally acceptable electrical power network that can be achieved with widespread applications of HTS power devices [17]. The cryogenic cooling capacity required for many HTS applications is rather large for a single cryocooler. As a consequence, multiple cryocoolers with heat exchangers and circulation pumps need to be integrated into a single system [18]. Cryocoolers have been used for HTS power applications. Most HTS power devices are cooled with liquid nitrogen and cryocoolers have been used to sub-cool liquid nitrogen that is circulated through the application. Many applications are designed to operate at temperatures below the liquid nitrogen temperature range (65 – 77 K) and require gaseous helium or neon in the circulation systems [19] [20]. One of the challenges with cryogenic gaseous circulation systems is that the pressure drop across the heat exchangers attached to the cryocoolers and the superconducting applications are high and the circulation pumps cannot handle the pressure drops at the required flow rates without losing extensive cooling capacity. Use of multiple cryocoolers and circulators is necessary for cryogenic helium circulation systems needed for many applications. Combining multiple units requires a thorough analysis to enable optimal designs [21]. This paper describes modelling efforts that would support the design of a versatile cryogenic helium circulation systems and the validation of the design parameters.

Cryocoolers 19, edited by S.D. Miller and R.G. Ross, Jr.

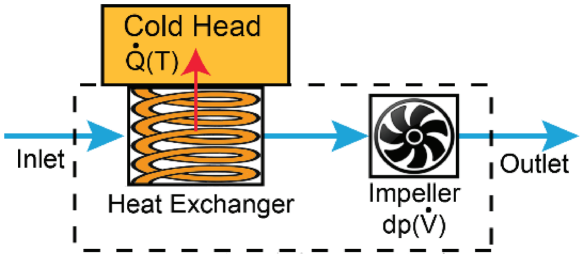

Figure 1. Schematic for one CHCS unit.

MODEL DESCRIPTION

Finite element method was used to analyze the cryogenic helium circulation system (CHCS) because it can handle complicated geometry in less time and with less effort than models developed using Fortran, Matlab, or Simulink. COMSOL Multiphysics® was used to develop the model. The built in Heat Transfer in Fluids physics module was coupled with the Low Reynolds Number k-epsilon Turbulent Flow physics where "Low Reynolds Number" refers to the fact that it resolves the boundary layer where the Reynolds number is significantly lower than the rest of the helium gas domain. The Reynolds number ranges from 50,000 to 125,000 and is within the turbulent regime. Only the helium domain is defined in the model, and the viscous dissipation is neglected. This domain consists of a heat exchanger followed by an internal impeller. Figure 1 shows a schematic of one CHCS which consists of a cryocooler, a heat exchanger (HX) and an impeller. The impeller is defined at an internal boundary that is perpendicular to the fluid flow. In addition, the impeller is characterized by a static pressure performance curve that is a function of the volumetric flow rate of the gaseous helium as shown in Figure 2 (a). This curve was defined within COMSOL in tabular form with a piece-wise cubic interpolation function. As the volumetric flow rate increases, the static pressure due to the impeller decreases.

The heat exchanger attached to the cold head in the gas flow stream has a smaller diameter than the rest of the CHCS resulting in a larger pressure drop due to friction. Comparable pressure drop is observed in the current heat exchangers tested at the Center for Advanced Power Systems (CAPS). The pressure drop through the heat exchanger on average is $\Delta p_{HX} = 4$ kPa. The boundary condition for the heat exchanger is characterized by the cooling power capacity curve of an AL325 Cryorefrigerator in which the cooling capacity is a function of the temperature of the cold head as shown in Fig 2 (b). A trend line with a second degree polynomial was generated from the power capacity curve, and it was applied to the interface between the cryocooler and heat exchanger in

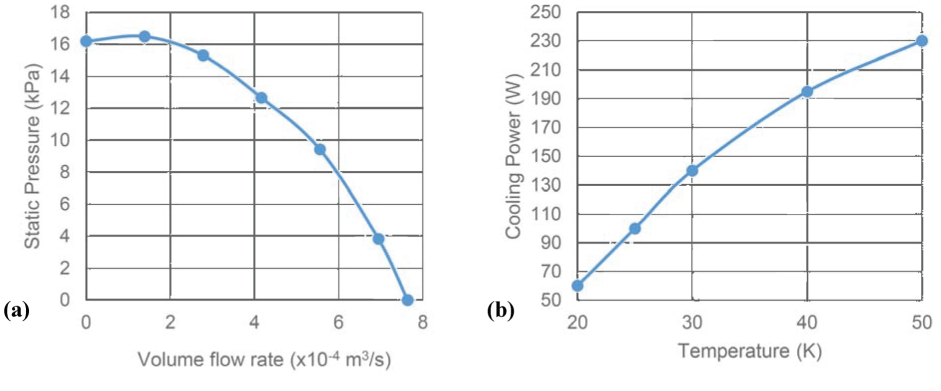

Figure 2. (a) Static pressure performance curve for CryoZone Noordwind CryoFan operating at 21,000 RPM. **(b)** Capacity curve for Cryomech AL325 cryocooler..

the CHCS. The boundary conditions for the entire model are as follows: inlet BC specifying mass flow rate, outlet BC specifying pressure, outward heat flux on the heat exchanger boundary, and all other boundaries are insulated. The heat capacity, viscosity, and thermal conductivity of helium are all functions of temperature, and the gas is considered ideal and compressible in order to calculate the density at each node in the mesh. The mesh of one CHCS unit contains 142,000 elements. The model was solved on a PC with an Intel i7-6700K processor and 32 GB of RAM running Windows 10. The former model description comprises one CHCS unit, and multiple units were added in series and/or parallel to analyze the relative performance of different configurations.

Figure 3 shows a few example configurations that were analyzed in this paper. The configurations denoted by parenthesis ( ) of interest are the following: two fans in series followed by two fans in parallel (1-1-2), one fan followed by two fans in parallel followed by one more fan (1-2-1), 2 fans in parallel followed by 2 fans in series (2-1-1), 2 fans in parallel followed by two more fans in parallel (2-2), and four fans in series (1-1-1-1). A parametric sweep of the mass flow rate between 6 g/s and 14 g/s was conducted while keeping the outlet pressure constant at 2 MPa for each configuration.

MODEL VERIFICATION

Before analyzing the various configurations of the 4 impeller system, the model had to be verified. This was done by running simulations on just one CHCS with the heat flux on the heat exchanger initially turned off. This provided the ability to test the behavior of the impeller and to determine if the gas can be assumed to be incompressible across the impeller. A further verification was made by adding another unit of CHCS in series and/or in parallel to see if these modifications behave similarly to that of a truly incompressible fluid. A final verification was made by turning on the heat flux and observing the temperature difference and density variation. Some of these verifications were also re-confirmed by manual calculations. All of these observations on the basic verifications are presented next.

For one case with a mass flow rate m. = 6 g/s at the temperature of 50 K, and the pressure before the impeller of p_i = 2 MPa, the model resulted in an increase in static pressure across the impeller of $\Delta p = p_o - p_i$ = 14.6 kPa, where subscripts i and o denote the property before and after the impeller, respectively. This result could easily be verified by manually calculating the volumetric flow rate and referring to the performance curve for the impeller from Figure 2(a) to find Δp. Equation (1) shows how the density before the first impeller was calculated.

$$\rho_i = \frac{p_i}{RT} \tag{1}$$

where R is the gas constant of helium, and *T* is the absolute temperature of the helium gas. The density before the impeller was used to calculate the volumetric flow rate shown in Equation (2).

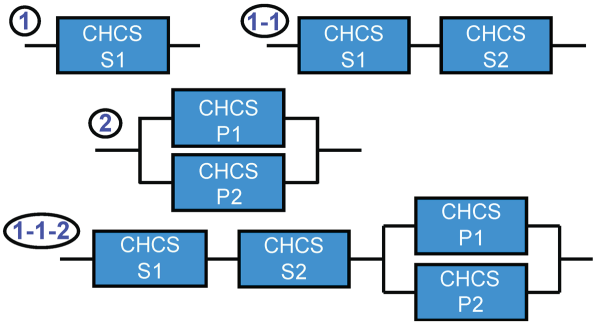

Figure 3. Examples of different configurations analyzed.

$$\dot{V}_i = \frac{\dot{m}}{\rho_i} \tag{2}$$

where $\dot{m}$ is the helium mass flow rate that is defined as the boundary condition at the inlet, the density before the impeller is $\rho_i \approx 19.26$ kg/m^3. This makes the volumetric flow rate before the impeller to be $\dot{V}_i \approx 3.12\text{x}10^{-4}$ m^3/s. By referencing the performance curve for the impeller, this volumetric flow rate corresponds to an increase in static pressure of $\Delta p \approx 14.7$ kPa. The error was within 0.7 %.

Another verification that was made was on the compressibility of the helium gas in our operational range. The density after the impeller is found using the following relationship.

$$\rho_o = \frac{p_o}{RT} \tag{3}$$

For the previous operational conditions, this results in a density after the impeller of $\rho_o \approx 19.4$ kg/m^3 which is an increase of only 0.7 %, and it verifies our assumption that helium gas can be assumed to be an incompressible fluid across the impeller. This is because the operational pressure is relatively high (2 MPa), and an increase in static pressure of only 15 kPa has almost no effect on the density. In addition, the process across the impeller is assumed to be adiabatic. Therefore, without cooling or heating, gaseous helium at high pressure may be treated as an incompressible fluid.

It is known that, for incompressible fluids, having two impellers in series will double the static pressure increase compared to that by one impeller. Additionally, having two impellers in parallel will double the mass flow rate and increase the static pressure by the same amount compared to that by one impeller. To ensure that the model will also provide the same result and for further validation, two additional cases were generated, one with two CHCS units in series (1-1) configuration and the other with two units of CHCS in parallel (2) configuration, both with heat transfer turned off. These results are shown in Figure 4, and they are as expected.

Finally, heat transfer was included in the model to verify the effects on the temperature of the helium. The heat flux that was applied to the outer boundary of the heat exchanger was initially set at a constant value of $\dot{Q}$= -200 W to simplify the verification. The model result shows a temperature difference through the heat exchanger of ΔT_{HX} = -6.3K. This can be verified by using a form of the first law of thermodynamics seen in Eq. (4).

$$\Delta T_{HX} = \frac{\dot{Q}}{\dot{m} C_p} \tag{4}$$

With $\dot{m}$ = 6 g/s and C_p = 5254 J/(kg K), Equation (4) gives ΔT_{HX} = -6.3K This verifies that the heat transfer physics within the model is accurate.

RESULTS

A parametric sweep was performed on the model for the mass flow rate from 6 – 14 g/s. To start, Figure 5 (a) shows how including nominal friction affects the increase in static pressure through

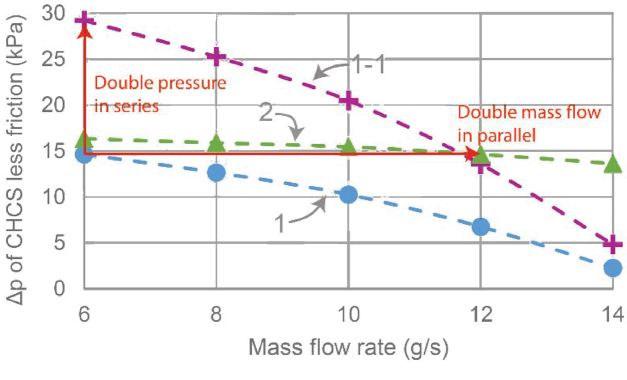

Figure 4. Increase in static pressure due to the impellers neglecting friction through the pipe.

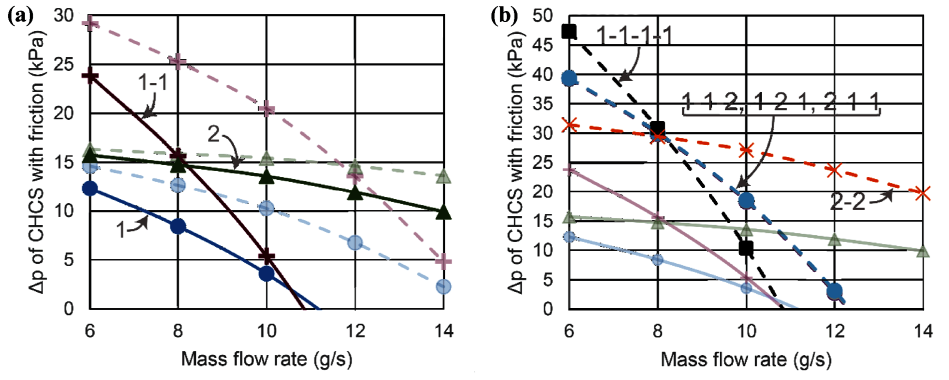

Figure 5. (a) Increase in static pressure vs. mass flow rate through cooling system with friction of the (1), (2), and (1-1) configurations (solid lines) compared to that without friction from Fig. 4 (transparent, dashed lines). **(b)** Increase in static pressure vs. mass flow rate through the cooling system for the four impeller configurations with friction (dashed lines) compared to the configurations with friction from Fig 5 (a) (transparent, solid lines). Note that this data is excluding the effects of heat transfer..

the cooling system. This is a necessary step in understanding the effects that friction has on each configuration and to provide clarity when designing a CHCS. The lengths of the tube channels were identical in all configurations. By including friction, the increase in static pressure of the (1) and (1-1) configurations dropped considerably more than that of the (2) configuration, and they can only provide flow rates up to 11 g/s. This is an example of a major drawback of the (1) and the (1-1) configurations. Many heat load applications require a flow rate of more than 8 g/s and the (2) configuration is the optimal choice. This shift occurs because having 2 impellers in parallel doubles the cross-sectional area of the flow channel providing less constriction and reduces the mass flow rate by half in each path. As the mass flow rate increases as in Figure 5 (a), the difference in the pressure drop between the (1-1) and (2) configurations increases exponentially. This is because the pressure drop due to friction is proportional to the square of the velocity.

To add even more complexity and versatility to the study, Figure 5 (b) shows the increase in static pressure of each of the four impeller configurations. The lines of the 4 different impeller configurations intersect at a mass flow rate of 8 g/s and a static pressure increase of 30 kPa. Another interesting result is that the combinations of two CHCS in series and two CHCS in parallel (1-1-2, 1-2-1, and 2-1-1) are all lined up. This implies that, with no cooling present, the total pressure drop is the sum of the individual pressure drops of each sub-scale CHCS configuration regardless of their order.

The following section presents the results that include heat transfer and friction for the various configurations with four impellers. Figure 6 (a) shows the increase in static pressure through the total cooling system for the four configurations with cryocoolers turned on (solid lines), and they are compared to the same configurations with cryocoolers turned off (transparent, dashed lines). The cryocoolers, when turned on, are removing heat from the helium gas and lower the temperature, which increases its density, and therefore the impellers perform better (refer to Figure 2). The configurations that benefit the most by adding heat transfer are (1-1-1-1) and (2-1-1). One of the most interesting observations of this analysis is how the relative performance of the various configurations, that have a combination of CHCS units in series and parallel, changes after including heat transfer and which configurations outperform the others. The (2-1-1) configuration performs slightly better than (1-2-1) and (1-1-2). This happens because the helium gas travels through the parallel section first where its density is increased more than that by a single CHSC, and this allows the following two CHCS units in series to produce higher static pressure. On the contrary, total temperature drop by the cooling system does not change with the configuration of CHCS units as long as the mass flow rate and the number of CHCS units are the same as shown in Figure 6 (b). In conclusion, the impeller performs better by decreasing the temperature first, but the ultimate temperature achieved by the cryogenic system remains unchanged regardless of the configuration of CHCS units.

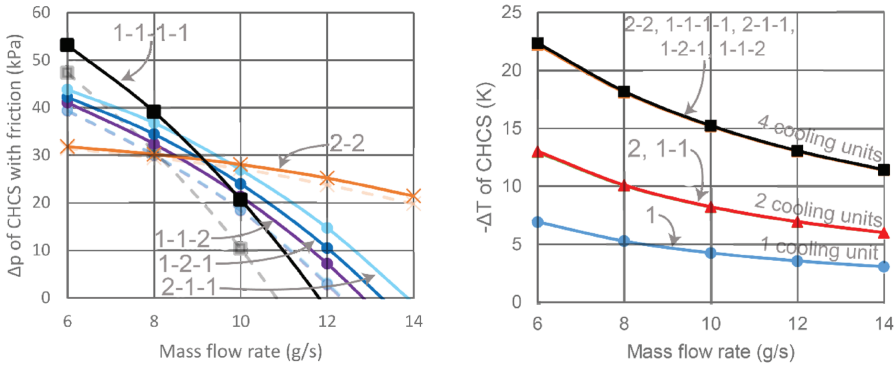

Figure 6. (a) Increase in static pressure vs. mass flow rate through cooling system for the four CHCS configurations including heat transfer through the heat exchanger (solid lines) compared to those without heat transfer (transparent, dashed lines). **(b)** Change in temperature of helium gas through the cooling system vs. mass flow rate for different CHCS unit configurations.

DISCUSSION

The modeling efforts described in this paper are necessary, educational, and beneficial for the development of versatile and optimized helium gas circulation systems. During the development of the model, it has been proven that gaseous helium may be assumed to be incompressible across the impeller, pipe friction affects the configurations of CHCS units that have more in series than in parallel, and that the orientation of the CHCS sub-scale configurations have no effect on the temperature differential through the cooling system (Figure 6 (b)).

The following discussion will present the process of choosing a CHCS configuration for an example set of specifications as a case study of the utility of the modelling. These specifications include a mass flow rate of $\dot{m} = 12$ g/s required to cool an HTS power cable that has a pressure drop of $\Delta p = 20$ kPa. Another requirement is that the cable system remain at or below $T = 50$ K, and the system load experiences a temperature rise of less than $\Delta T = 7.5$ K. Looking at Figure 7, it appears that, in order to get a temperature difference of $\Delta T = 7.5$ K and a mass flow rate of $\dot{m} = 12$ g/s, it is required to have more than two CHCS units. It is possible to use just three CHCS units in this case, but these configurations were omitted in this analysis, and one of the configurations with four CHCS units will be chosen. Figure 6 will help in selecting one of the specific configurations among the possible four unit options. For a pressure drop of $\Delta p = 20$ kPa and mass flow rate of $\dot{m} = 12$ g/s, only the (2-2) configuration is capable of satisfying the required operational specifications. This is a generic design, but the (2-2) configuration appears to be the optimal configuration of CHCS units in parallel and series for most large-scale HTS applications.

Another important factor to consider when designing a set of multiple CHCS units is the friction. Here, pipe length and diameter are important parameters. It has been observed in previous experimental results that parallel channels with different pipe lengths produce undesirable effects such as backflow. Also, having parallel channels converge to a single channel with the same diameter creates flow constriction.

This model will be used in the future design of an experimental cryogenic helium circulation system where the different configurations of four CHCS units will be tested and the performances compared to that of the model results. Figure 7 shows an example of a (2) configuration setup that will be tested and compared to the FEM model. The lessons of pipe friction and performance of different configurations will be applied to the experiment to aid in designing a versatile gaseous helium cryogenic systems needed for supporting many different types of HTS applications.

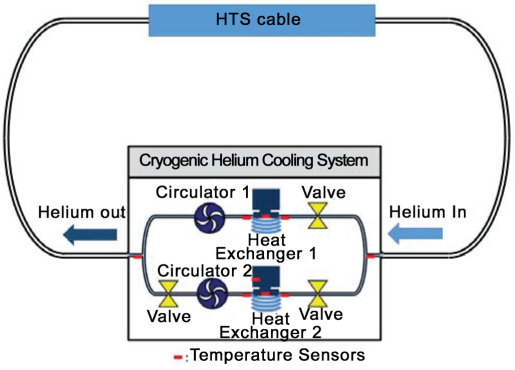

Figure 7. Physical system schematic used for experimental validation of CHCS FEM model.

ACKNOWLEDGMENTS

This work was sponsored by the US Office of Naval Research under contract N000141410198.

REFERENCES

1. Grant, P. M., Starr, C., and Overbye, T. J., "A power grid for the hydrogen economy," *Scientific American*, 295(1), pp. 76-83.
2. Trevisani, L., Fabbri, M., and Negrini, F., "Long-term scenarios for energy and environment: Energy from the desert with very large solar plants using liquid hydrogen and superconducting technologies," *Fuel processing technology* 87, no. 2 (2006): 157-161.
3. Haugan, T. J., Long, J. D., Hampton, L. A., & Barnes, P. N. "Design of compact, lightweight power transmission devices for specialized high power applications," *SAE International Journal of Aerospace* 1, no. 2008-01-2930 (2008): 1088-1094.
4. Ballarino, A., "Design of an MgB2 feeder system to connect groups of superconducting magnets to remote power converters," *Journal of Physics: Conference Series*, vol. 234, no. 3, p. 032003. IOP Publishing, 2010.
5. Rey, C. M., Duckworth, R. C., Demko, J. A., Ellis, A., James, D.R., Gouge, M. J., "Test results for a 25 meter prototype fault current limiting HTS Cable for project Hydra," *Adv. in Cryogenic Engineering*, AIP Publishing, 2010: 453-460.
6. Ferrara, P. J., Uva, M. A., and Nowlin, J., "Naval ship-to-shore high temperature superconducting power," *IEEE Transactions on Applied Superconductivity* 21, no. 3 (2011): 984-987.
7. Kalsi, S. S., *Applications of high temperature superconductors to electric power equipment*, John Wiley & Sons, 2011.
8. van der Laan, D. C., Lu, X. F., & Goodrich, L. F., "Compact GdBa2Cu307-o coated conductor cables for electric power transmission and magnet applications Contribution of NIST, not subject to US copyright," *Superconductor Science and Technology* 24, no. 4 (2011): 042001.
9. Maguire, J. F., Yuan, J., Romanosky, W., Schmidt, F., Soika, R., Bratt, S., "Progress and status of a 2G HTS power cable to be installed in the long island power authority (LIPA) grid," IEEE Transactions on Applied Superconductivity 21, no. 3 (2011): 961-966.
10. Gamble, B., Snitchler, G., & MacDonald, T., "Full power test of as 36.5 MW HTS ship propulsion motor," *IEEE Transactions on Applied Superconductivity* 21, no. 3 (2011): 1083-1088.
11. Ohsaki, H., Lv, Z., Sekino, M., & Tomita, M., "Application of superconducting power cables to DC electric railway systems," *Physics Procedia* 36 (2012): 908-913.
12. Ryu, C., Jang, H., Choi, C., Kim, Y., Kim, H. "Current status of demonstration and commercialization of HTS Cable system in grid in Korea," *Applied Superconductivity and Electromagnetic Devices (ASEMD), 2013 IEEE International Conference on*, pp. 539-542. IEEE, 2013.
13. Xiao, L., Dai, S., Lin, L., Zhang, Z., & Zhan, J., "HTS power technology for future DC power grid," *IEEE Transactions on Applied Superconductivity* 23, no. 3 (2013): 5401506-5401506.

14. Dai, S., Xiao, L., Zhang, H., Teng, Y., Liang, X., Song, N., “Testing and demonstration of a 10-kA HTS DC power cable,” *IEEE Transactions on Applied Superconductivity* 24, no. 2 (2014): 99-102.
15. Stemmle, M., Merschel, F., Noe, M., and Hobl, A., "AmpaCity - Advanced superconducting medium voltage system for urban area power supply," In *2014 IEEE PES T&D Conference and Exposition*, pp. 1-5. IEEE, 2014.
16. Morandi, A., “HTS dc transmission and distribution: concepts, applications and benefits,” *Superconductor Science and Technology* 28, no. 12 (2015): 123001.
17. Radebaugh, R., “Cryocoolers: the state of the art and recent developments,” *Journal of Physics: Condensed Matter* 21, no. 16 (2009): 164219.
18. Pamidi, S. V., Kim, C. H., Kim, J-h., Crook, D., & Dale, S., “Cryogenic helium gas circulation system for advanced characterization of superconducting cables and other devices,” *Cryogenics* 52, no. 4 (2012): 315-320.
19. Saji, N., Asakura, H., Yoshinaga, S., Ishizawa, T., Miyake, A, Obata, M., “Design of oil-free simple turbo type 65 K/6 kW helium and neon mixture gas refrigerator for high temperature superconducting power cable cooling,” *Adv. in Cryogenic Engineering: Proceedings of the Cryogenic Engineering Conference-CEC*, vol. 613, no. 1, pp. 893-902, AIP Publishing, 2002.
20. Zhang, T., Haran, K., Laskaris, E.T., Bray, J. W., “Design and test of a simplified and reliable cryogenic system for high speed superconducting generator applications,” *Cryogenics* 51, no. 7 (2011): 380-383.
21. Suttell, N., Kim, C. H., Ordonez, J., Kephart, J., Graber, L., Pamidi, S., “Three-dimensional finite-element analysis of terminations for gaseous-helium-cooled high-temperature superconducting power cables,” *IEEE Transactions on Applied Superconductivity* 26, no. 4 (2016): 1-5.